Performance of Flocking-Based Control Schemes in Smart Grid Applications

Abdallah K. Farraj Eman M. Hammad Jin Wei Deepa Kundur Karen L. Butler-Purry†
Department of Electrical and Computer Engineering, University of Toronto, Toronto, Ontario, Canada
†Department of Electrical and Computer Engineering, Texas A&M University, College Station, Texas, USA
Email: {abdallah, ehammad, jinwei, dkundur}@ece.utoronto.ca, klbutler@tamu.edu

***Abstract*—Flocking control has recently been used in smart grid applications to stabilize power systems during a transient instability period. Based on consensus and cooperation of multi-agent control systems, flocking control uses cyber information about the power system to help achieve stability after the occurrence of a fault in the power system. Recent work showed that such controller can be useful in a smart power grid; however, issues of the controller's power usage, stability time, and frequency deviation have not been investigated yet. This paper investigates the effect of the power generators' inertia on these issues in a WECC 3-generator power system. Results of this work show that the location of the fault affects the relationship between the generators' inertia and the investigated measures.**

I. Introduction

Interest in smart grid systems has surged recently. Smart grid systems use advanced control, communications, and sensor technologies to improve the efficiency and resilience of the power grid. Further, smart grid technologies can help utility companies to better manage and control the energy resources and meet the customers' demand. In addition, the increasing integration of renewable energy sources and storage units into the power grid accelerates the interest of adopting smart grid technologies.

The cyber assets of a smart grid include communication and information technology infrastructures, computing systems, and data storage units. Cyber data can be collected over the power grid using phasor measurements units (PMUs) and remote terminal units (RTUs); this data can be transferred, as an example, to supervisory control and data acquisition (SCADA) systems using fiber optics communication links. The timely availability of the system's cyber data can help a control center better stabilize the power system.

A flocking-based control is a nonlinear control that is based on consensus and cooperation of multi-agent control systems. In general, a flocking scheme can be used to control flockmates (or agents) to achieve [1], [2]:

- flock centering where an agent stays close to nearby agents;
- collision avoidance where an agent avoids colliding with nearby agents; and
- velocity matching where an agent attempts to match the speed of nearby agents.

For a power system application, the flock centring feature can be used to achieve phase angle cohesiveness while the velocity matching feature can be used to achieve frequency synchronization between the generators of the power system. A recent work in [3]–[6] employed the concepts of flocking control to aid the generators achieve stability during a transient instability period.

The proposed flocking controller employs the cyber information about the system into a nonlinear controller to help the power system achieve stability after the occurrence of a fault in the power grid. A local controller is used for each generator, and an external, fast-acting, power source is employed by each controller. The goal of the controller is to achieve frequency stability and phase cohesiveness when the power system undergoes a transient instability.

Although the work of [3]–[7] shed a light on the application of flocking control for smart grids, the impact of having different generators' parameters on the performance of the controller was not investigated. Further, some performance measures were not considered. For example, the stability time of the system generators, the average power used by the controller, and the frequency deviation of the generators have not been investigated yet.

This paper investigates the performance of the flocking control in a smart grid application. Specifically, this work explores the effect of the inertia of the power generators on the power usage, stability time, and average frequency for a WECC 3-generator power system.

The rest of this paper is organized as follows. System model is shown in Section II. Section III investigates the performance of the flocking control. Conclusions and final remarks are shown in Section IV.

II. System Model

Flocking-based control can be used to achieve transient stability in case of a fault in the power system. In this setup, a local controller is used for each generator and an external power source is employed by each controller.

A schematic of the WECC 3-generator power system is shown in Fig. 1. In this power system, Bus 1 is the slack bus, Buses 2 and 3 are PV buses, and Buses 7 and 8 are PQ (load) buses. The parameters of the power system's generators are shown in Table I, where M_i and D_i are expressed in seconds, δ_i is expressed in radians per second, and the rest are expressed in per units.

The swing equation links the system parameters in a differential equation, and it can be used to study the transient

978-1-4799-7088-9/14/$31.00 ©2014 IEEE

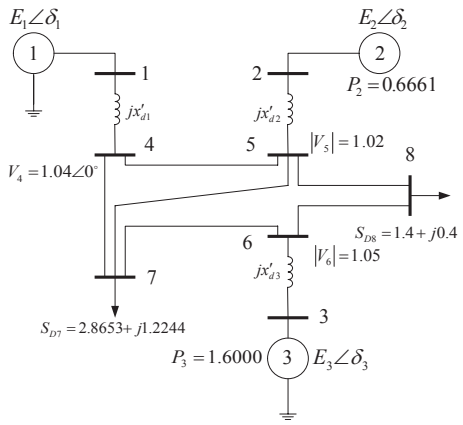

Fig. 1. WECC power system model

stability of a power system. Further, during the transient instability duration, the system parameters can be considered constant. Consequently, a swing equation with time-invariant parameters can be used to model the power system dynamics during the transient instability period.

Parameter	Description
E_i	internal voltage of Generator i, $i = 1, \ldots, N$
$P_{e,i}$	electrical power of Generator i
$P_{m,i}$	mechanical power of Generator i
M_i	inertia of Generator i
D_i	damping constant of Generator i
δ_i	rotor angle of Generator i
ω_i	relative normalized rotor frequency of Generator i
X'_{di}	direct-axis transient reactance of Generator i
G_{ii}	equivalent shunt conductance of Generator i

TABLE I
SYSTEM PARAMETERS

Let $\dot{\delta}_i$ and $\dot{\omega}_i$ denote the derivatives of δ_i and ω_i with respect to time, respectively, then the swing equation of an interconnected power system is expressed as [8], [9]

$$\begin{aligned} \dot{\delta}_i &= \omega_i \\ \dot{\omega}_i &= -\tfrac{D_i}{M_i}\,\omega_i + \tfrac{1}{M_i}\left(P_{m,i} - P_{e,i}\right), \end{aligned} \tag{1}$$

where the electrical power of Generator i is defined as

$$P_{e,i} = \sum_{k=1}^{N} |E_i|\,|E_k|\,\left[G_{ik}\cos\left(\delta_i - \delta_k\right) + B_{ik}\sin\left(\delta_i - \delta_k\right)\right], \tag{2}$$

where N is the number of generators in the power system, $G_{ik} = G_{ki} \geq 0$ is the Kron-reduced equivalent conductance between Generators i and k, $B_{ik} = B_{ki} > 0$ is the Kron-reduced equivalent susceptance between Generators i and k, and $Y_{ik} = G_{ik} + \sqrt{-1}\,B_{ik}$ is the Kron-reduced equivalent admittance between Generators i and k. All of Y_{ik}, G_{ik}, and B_{ik} are expressed in per unit values. Using $\phi_{ik} = \arctan\left(\frac{G_{ik}}{B_{ik}}\right)$ and $P_{ik} = |E_i||E_k||Y_{ik}|$, then the swing equation is reduced into

$$\begin{aligned} \dot{\delta}_i &= \omega_i \\ \dot{\omega}_i &= -\tfrac{D_i}{M_i}\,\omega_i + \tfrac{1}{M_i}\left(P_{m,i} - |E_i|^2\,G_{ii}\right) \\ &\quad -\tfrac{1}{M_i}\sum_{k=1,k\neq i}^{N} P_{ik}\,\sin\left(\delta_i - \delta_k + \phi_{ik}\right). \end{aligned} \tag{3}$$

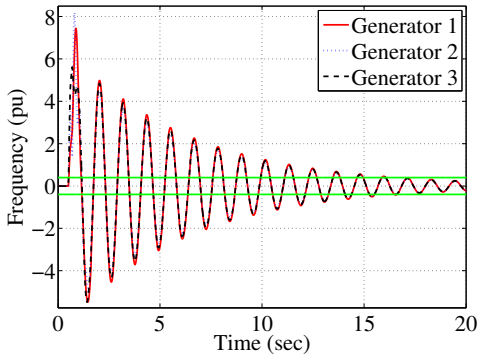

Fig. 2. Relative normalized frequency of the system generators

Without a governor control, as described in Eqs. (1) and (3), the generators cannot stabilize the power system whenever there is a fault in any bus in the system. However, using external controllers can help stabilize the power system during the transient instability period. Applying an external power at Generator i, termed as U_i, changes the swing equation into

$$\begin{aligned} \dot{\delta}_i &= \omega_i \\ \dot{\omega}_i &= -\tfrac{D_i}{M_i}\,\omega_i + \tfrac{1}{M_i}\left(P_{m,i} - |E_i|^2\,G_{ii}\right) \\ &\quad -\tfrac{1}{M_i}\sum_{k=1,k\neq i}^{N} P_{ik}\,\sin\left(\delta_i - \delta_k + \phi_{ik}\right) + \tfrac{1}{M_i}U_i\,. \end{aligned} \tag{4}$$

In a flocking-based control, U_i can be used to achieve both frequency synchronization and phase cohesiveness between the system generators. Specifically, U_i is calculated as [3]

$$\boldsymbol{U} = \sum_{\substack{k=1\\k\neq i}}^{N}\left[\int_{t_0}^{t}\rho(\delta_i - \delta_k)\,\mathrm{d}t\right]\mathbf{1} - \boldsymbol{G\delta} - \boldsymbol{B\omega} \cdot \boldsymbol{D} - c(\boldsymbol{\delta} - \boldsymbol{\delta_0}), \tag{5}$$

where $\boldsymbol{U} = [U_1, U_2, \ldots, U_N]^T$, t_0 is the time to activate the flocking control, t is the time to calculate the value of the control, ρ is a control function, c is a navigation term, $\boldsymbol{\delta_0} = [\delta_{0_1}, \delta_{0_2}, \ldots, \delta_{0_N}]^T$ are the phase values at t_0, $\boldsymbol{D} = [D_1, D_2, \ldots, D_N]^T$, $\boldsymbol{\delta} = [\delta_1, \delta_2, \ldots, \delta_N]^T$, and $\boldsymbol{\omega} = [\omega_1, \omega_2, \ldots, \omega_N]^T$. Moreover, $\boldsymbol{B}$ and $\boldsymbol{G}$ are cyber control matrices.

It is noted that the model of the local generators does not include a governor control. The presence of a governor controller helps the generator during the instability duration; however, the governor control is much slower than the flocking controller. Consequently, it is believed that if the flocking controller stabilizes the system without the governor control, the power system will also be stable when the governor control is activated.

III. Evaluation of Flocking Control

The impact of the generators' inertia on the flocking controller's performance is investigated in this section. Specifically, the stability time and the average frequency of the power system's generators, and the average external power needed by the controller are considered. The WECC 3-generator test system is simulated to demonstrate the effectiveness of the flocking control.

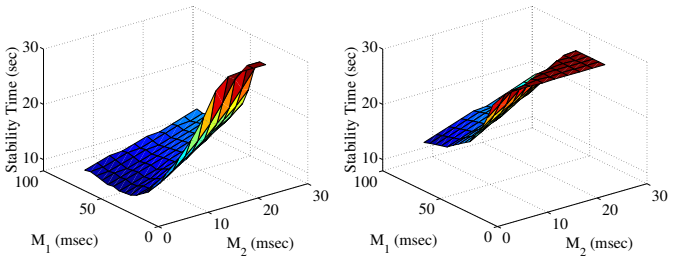

(a) M_3 = 25 msec (b) M_3 = 50 msec

Stability time of Generator 1

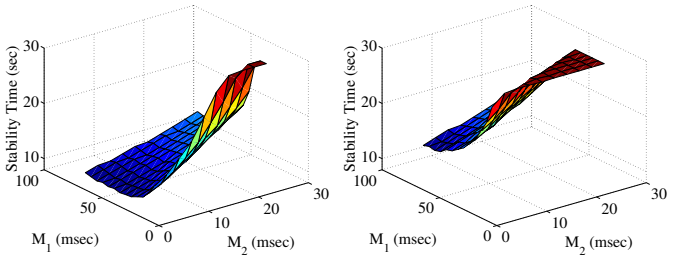

(c) M_3 = 25 msec (d) M_3 = 50 msec

Stability time of Generator 2

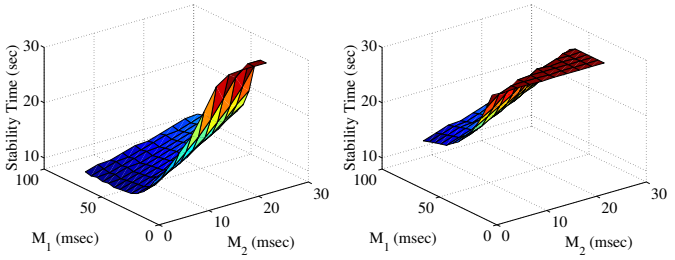

(e) M_3 = 25 msec (f) M_3 = 50 msec

Stability time of Generator 3

Fig. 3. Stability time of the system generators

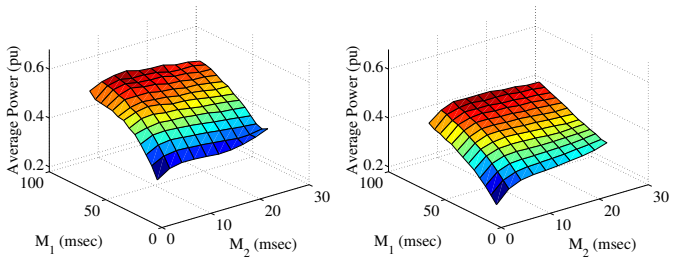

(a) M_3 = 25 msec (b) M_3 = 50 msec

Average power of U_1

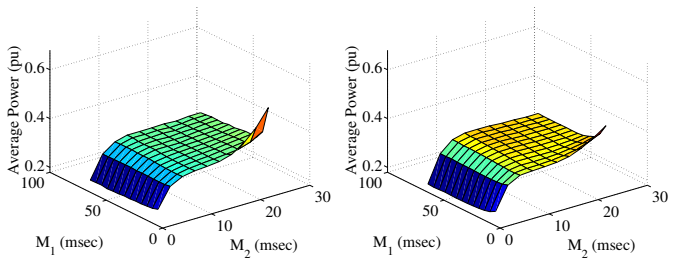

(c) M_3 = 25 msec (d) M_3 = 50 msec

Average power of U_2

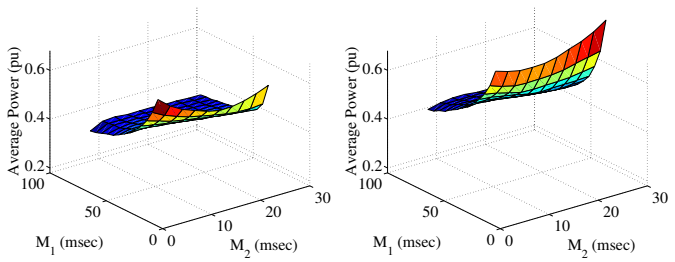

(e) M_3 = 25 msec (f) M_3 = 50 msec

Average power of U_3

Fig. 4. Average external power needed by the flocking controller

As shown in Fig. 1, N = 3 for the 3-generator power system. Let D_1 = 0.005 seconds, D_2 = 0.001 seconds, D_3 = 0.002 seconds, X'_{d1} = 0.08 pu, X'_{d2} = 0.18 pu, and X'_{d3} = 0.12 pu. The value of M_1 is varied between 15 to 75 msec, M_2 is varied between 2.5 to 25 msec, and the value of M_3 is alternated between 25 and 50 msec.

Running the load flow analysis for the power system before the fault occurs yields E_1 = 1.162 $\angle 7.605°$, E_2 = 1.261 $\angle -8.904°$, and E_3 = 1.244 $\angle -4.024°$. Because the power system is balanced and there are no transients before the fault, the mechanical power for each generator equals its electrical power. Consequently, using Eq. (2), the values of the mechanical power for each generator, in per unit values, are $P_{m,1}$ = 1.9989, $P_{m,2}$ = 0.6661, and $P_{m,3}$ = 1.6.

The power system is assumed to be running normally from t = 0 to t = 0.5 seconds. However, a 3-phase fault occurs at Bus 6 at t = 0.5 seconds. Then, Line 6-7 is tripped out to clear the fault at t = 0.6 seconds. Finally, the flocking controller is activated on all generators from t = 0.7 seconds to t = 30 seconds.

Stability time of a generator is found by finding the time after which the relative normalized frequency of the generator is restricted to some threshold (called stability margin). For M_1 = 50 msec, M_2 = 15 msec, and M_3 = 35 msec, Fig. 2 displays the relative normalized frequency of the three generators. It is noted that when the stability margin is set to 0.4, the three generators need slightly more than 16 seconds to stabilize.

Stability time results of the three generators are shown in Fig. 3. It is noted that the stability time increases with increasing the inertia of Generator 2. Moreover, when M_3 increases, the stability time is expected to increase as well. For Generator 1 (the slack generator), the stability time decreases with increasing the inertia up to a point, then the stability time levels off (or increases slightly).

The simulation results show that the lowest stability times are 9.27 seconds for Generator 1 (when M_1 = 45 msec, M_2 = 2.5 msec, and M_3 = 25 msec); 8.75 seconds for Generator 2 (when M_1 = 45 msec, M_2 = 2.5 msec, and M_3 = 25 msec); and 9.07 seconds for Generator 3 (when M_1 = 50 msec, M_2 = 2.5 msec, and M_3 = 25 msec). However, the flocking controller cannot stabilize the power system in some cases within the 30-second run. Specifically, for low values of M_1 and high values of M_2 and M_3, the power system appears slower in

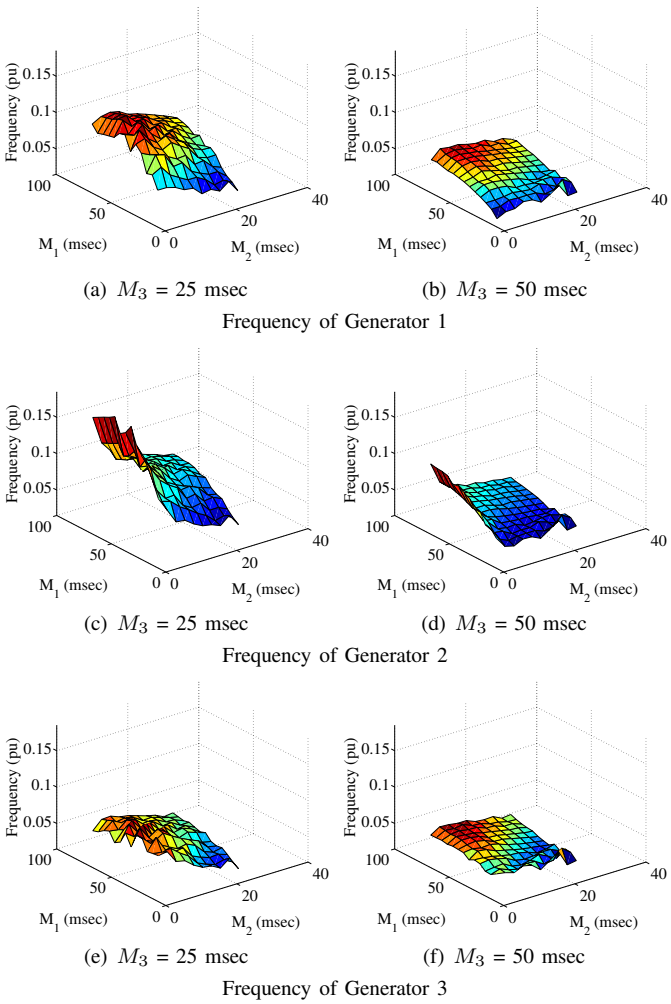

(a) M_3 = 25 msec (b) M_3 = 50 msec

Frequency of Generator 1

(c) M_3 = 25 msec (d) M_3 = 50 msec

Frequency of Generator 2

(e) M_3 = 25 msec (f) M_3 = 50 msec

Frequency of Generator 3

Fig. 5. Relative normalized frequency of the system generators

responding to the flocking controller. With doubling the inertia of Generator 3, the number of cases that the generators in the power system cannot be stabilized increases as seen in Table II.

The flocking control relies on external power sources (U_i, where $i = 1, \ldots, N$) to stabilize the power system as shown in Eq. (4). The value of $\boldsymbol{U}$ is calculated according to Eq. (5).

Fig. 4 displays the average external power needed by the flocking controller during the time when the controllers are activated. It is observed that with increasing M_1, the controller needs more power to stabilize Generator 1 and less power to stabilize Generator 3. On the other hand, increasing the inertia of Generator 2 causes the flocking controller to use more external power for the three generators (the increase is less obvious for Generator 3). Further, Table III shows some results for M_3, where an increase in inertia means more external power is needed to stabilize Generator 3 and less power to stabilize Generator 1.

Finally, Fig. 5 shows the average relative normalized frequency of the system's generators during the controllers' active time. One goal of the flocking control is to achieve exponential frequency synchronization through $\lim_{t\to\infty} \omega_i(t) = 0$. Consequently, it is preferred that the relative normalized frequency of the system generators be as close as possible to zero.

	M_3 = 25 msec	M_3 = 50 msec
Generator 1	3.08%	15.39%
Generator 2	3.08%	14.62%
Generator 3	3.08%	19.23%

TABLE II
PERCENTAGE OF CASES WHERE THE GENERATOR IS NOT STABILIZED

	M_3 = 25 msec	M_3 = 50 msec
Generator 1	0.4890	0.3933
Generator 2	0.3154	0.3120
Generator 3	0.4608	0.5704

TABLE III
AVERAGE EXTERNAL CONTROL POWER (PU)

	M_3 = 25 msec	M_3 = 50 msec
Generator 1	0.0799	0.0415
Generator 2	0.0933	0.0493
Generator 3	0.0547	0.0429

TABLE IV
AVERAGE RELATIVE NORMALIZED FREQUENCY (PU)

As the value of M_1 increases, the average values of ω_1 and ω_3 increase. However, increasing the value of M_2 decreases the average values of the frequency. Further, Table IV shows the relationship between M_3 and the average frequency. When the value of M_3 is increased, both average values of ω_1 and ω_2 decrease.

It is observed that the location of the 3-phase fault and the tripped out line (i.e., Line 6-7) affects the way the generators respond to the flocking control. Specifically, it is shown that the inertia of Generator 3 (with its close proximity to Line 6-7) has the most effect on the stability time of the generators of the power system.

IV. CONCLUSIONS

Flocking control was recently proposed to help achieve transient stability after the occurrence of a fault in the power system. This paper investigates performance aspects of flocking-based control for power systems. Specifically, this work explores the relation between the inertia of the system generators and the stability time, the external control power, and the system frequency.

Results of this work show that the location of the fault affects the way the flocking controllers perform. Further, the value of the inertia of the generator that is closest to the faulted line has the most impact on the performance of the controller.

ACKNOWLEDGMENT

This work was supported by the Natural Sciences and Engineering Research Council of Canada and the U.S. National Science Foundation under grant ECCS-1028246. The authors acknowledge the contributions of Blas Sanchez in preparing the simulation environment.

REFERENCES

[1] C. W. Reynolds, "Flocks, Herds, and Schools: A Distributed Behavioral Model," in *Annual Conference on Computer Graphics and Interactive Techniques – Computer Graphics*, vol. 21, pp. 25–34, July 1987.

[2] R. Olfati-Saber, "Flocking for Multi-Agent Dynamic Systems: Algorithms and Theory," *IEEE Transactions on Automatic Control*, vol. 51, pp. 401–420, March 2006.

[3] J. Wei, D. Kundur, T. Zourntos, and K. L. Butler-Purry, "A Flocking-Based Dynamical Systems Paradigm for Smart Power System Analysis," in *IEEE Power and Energy Society General Meeting (PESGM)*, pp. 1–8, 2012.

[4] J. Wei and D. Kundur, "Two-Tier Hierarchical Cyber-Physical Security Analysis Framework For Smart Grid ," in *IEEE Power and Energy Society General Meeting (PESGM)*, pp. 1–5, 2012.

[5] J. Wei, D. Kundur, and T. Zourntos, "On the Use of Cyber-Physical Hierarchy for Smart Grid Security and Efficient Control," in *IEEE Canadian Conference on Electrical and Computer Engineering (CCECE)*, pp. 1–6, 2012.

[6] J. Wei, D. Kundur, T. Zourntos, and K. L. Butler-Purry, "Probing the Telltale Physics: Towards a Cyber-Physical Protocol to Mitigate Information Corruption in Smart Grid Systems," in *IEEE International Conference on Smart Grid Communications (SmartGridComm)*, pp. 372–377, 2012.

[7] A. K. Farraj, E. M. Hammad, J. Wei, D. Kundur, and K. L. Butler-Purry, "Performance Evaluation of Flocking-Based Distributed Cyber-Physical Control for Smart Grid," in *IEEE International Conference on Smart Grid Communications (SmartGridComm)*, pp. 1–6, 2014.

[8] F. Dörfler and F. Bullo, "Synchronization and Transient Stability in Power Networks and Non-Uniform Kuramoto Oscillators," in *American Control Conference (ACC)*, pp. 930–937, 2010.

[9] P. M. Anderson and A. A. Fouad, *Power System Control and Stability*. IEEE Power Systems Engineering Series, Piscataway, NJ: IEEE Press, 1994.